Losses In Solid Oxide Fuel Cells Different Materials

Araniya K. K.[1]**, Nayak H. B.**[2]**, Gajjar V. Y.**[3]**, Patel A. D.**[4]
[1,2](Assistant Professor in Mechanical Engineering Department, Faculty of Engineering Technology & Research, Isroli-Afwa,Bardoli,
[3](Assistant Professor in Mechanical Engineering Department, SVMIT,Bharuch).
[4](PG Student in Mechanical Engineering Department, SVMIT,Bharuch)

Abstract

Engineers and environmentalists have long dreamed of being able to obtain the benefits of clean electric power without pollution-producing engines or heavy batteries. Solar panels and wind farms are familiar images of alternative energy technologies. While they are effective sources of electrical energy, there are problems with the stability of their energy source as, on a cloudy or windless day. Their applications are somewhat limited due to lack of portability; a windmill is not much help to the power plant of a diesel truck, a solar panel cannot provide power at night, etc. Much development has focused on solid oxide fuel cells (SOFC), both because they are able to convert a wide variety of fuels and because they do so with High efficiency compared to engines and modern thermal power plants fuel cells have potentially higher energy density than batteries and promise a significant increase in power availability. In this paper, find out Activation Losses, Concentration Losses, Internal Current Losses, Ohmic Losses and which losses are more significant.

Keywords – Activation Losses, Concentration Losses, Internal Current Losses, Ohmic Losses, Solid Oxide Fuel Cells,

Introduction

In 1962 a revolution in energy research occurred. Scientists at Westinghouse Electric Corporation demonstrated for the first time the feasibility of extracting electricity from a device they called a "solid electrolyte fuel cell since then there has been an intense research and development effort to develop the alternative energy technology known as fuel cells. Now, as energy issues are at the front of current events, fuel cell technology is ripening and on the border of being ready for large scale commercial implementation. Fuel cells are electrochemical devices that convert the chemical energy of a reaction directly into electrical energy. The basic physical structure or building block of a fuel cell consists of an electrolyte layer in contact with a porous anode and cathode on either side. A schematic representation of a fuel cell with the reactant / product gases and the ion conduction flow directions through the cell is shown in Fig.1. In a typical fuel cell gaseous fuels are feed continuously to the anode (negative electrode) compartment and an oxidant (i.e., oxygen from air) is fed continuously to the cathode (positive electrode) compartment; the electrochemical reactions take place at the electrodes to produce an electric current. A fuel cell although having components and characteristics similar to a typical battery but differs in several respects. The battery is an energy storage device. The maximum energy available is determined by the amount of chemical reactant stored within the battery itself. The battery will cease to produce electrical energy when the chemical reactants are consumed (i.e., discharged). In a secondary battery, the reactants are regenerated by recharging, which involves putting energy into the battery from an external source. The fuel cell is an energy conversion device that theoretically has the capability of producing electrical energy for as long as the fuel and oxidant are supplied to the electrodes. Fig.2 is a simplified diagram that demonstrates how the fuel cell works.

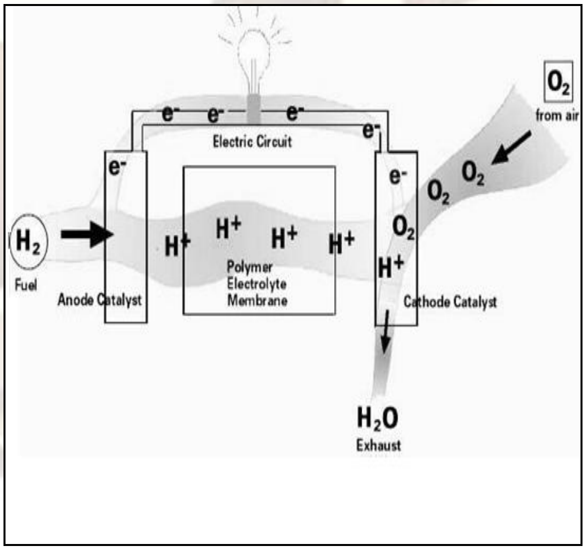

Fig. 1 Working of fuel cell

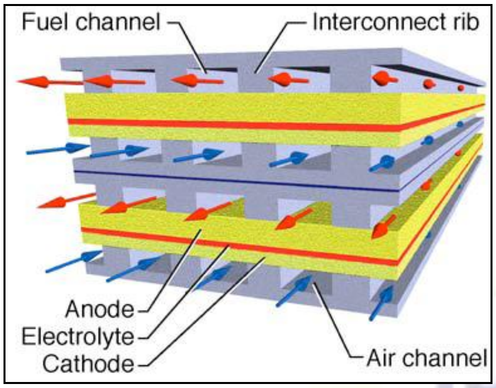

Fig. 2 Basic arrangement of fuel cell

I. LITERATURE REVIEW

Fuel cell hardware is presently in pre-commercial development stage, it resulting in the unavailability of performance maps for system design and simulation purposes. Consequently, prediction of fuel cell performance is highly dependent on modeling.

Lukas et al., [5] and Domergue et al., [6] have proceeded to model dynamic fuel cell performance using zero-dimensional, single node lumped models.

Comte et al., [7] emphasized that zero-dimensional models cannot accurately simulate dynamic fuel cell performance, particularly those employing internal steam reforming. In fact, the authors claim that errors of 20% (relative to more complex models) are possible in predicting the fuel cell thermal and power outputs using zero-dimensional models for cross-flow configurations.

Debendetti and Vayenas [4] were the first to model flat planar SOFCs. These authors developed a 2-D modeling approach still in use today, which approximates the cell stack as set of unit cells operating as continuously stirred tank reactors.

Ahmed, et al., [1] developed a 2-D model of a monolithic cell following a similar approach as the unit cell approximation described previously.

Hartvigsen et al., [2] developed a 3D finite element model incorporating conduction, convection, and radiation heat transfer mechanisms in a single cell channel.

Karoliussen [3] advanced the previous steady-state models by developing a 3-D model that accounted for internal reforming and incorporating a more complete description of all heat and mass transfer processes including interaction of the stack with its surroundings.

Hirano et al. [8] assumed that the anode gases were nearly transparent to the thermal radiation because of the small distances between tubes. There was no mention of radiation heat transfer between the cells and the containing walls, which would be a larger distance and a larger temperature difference. Radiation was assumed to be a negligible means of heat transfer compared to convection and thus ignored. In general all SOFC systems research in the open literature is model-based, consisting of only fuel cell stack and reformer component models (no system-level simulation), both of which have yet to be experimentally validated. Additionally, due to the number of different SOFC designs (tubular, radial planar, flat planar {electrode-supported and anode supported}) being developed, the results of one study may be limited or not applicable to all SOFC systems in use.

Achenbach [9] showed that a significant amount (5 KW/m2) of energy would be radiated from a planar stack if the temperature difference between the cell and the vessel wall was only 10°C. Radiation effects were not considered within the cells.

II. FUEL CELL MODELING

Modeling plays a significant and important role in fuel cell design and development process. A fundamental fuel cell model consists of five principles of conservation: mass, momentum, species, charge, and thermal energy. These transport equations are then coupled with electrochemical processes through source terms to describe reaction kinetics. Typically the fuel cell to be modeled is schematically shown in Fig. 7 and divided into seven sub regions: the anode gas channel, anode gas diffusion layer (GDL), anode catalyst layer, ionomeric membrane, cathode catalyst layer, cathode gas diffusion layer (GDL), and cathode gas channel.

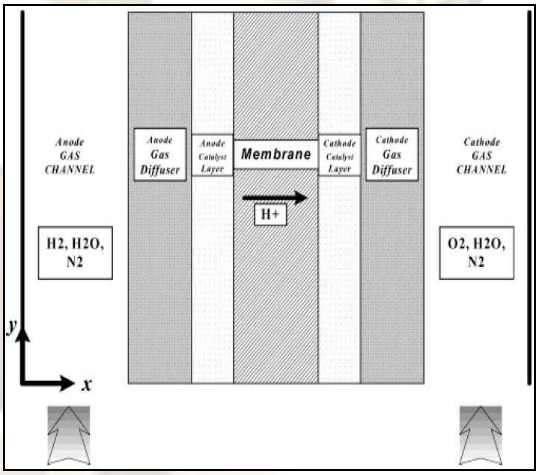

Fig. 3 Fuel Cell sub regions for CFD model

All components of the fuel cell must have similar thermal expansion in order to minimize thermal stresses, which may cause cracking and de-lamination during thermal cycling. In addition, the components must be chemically stable in order to limit chemical interactions with other cell components.

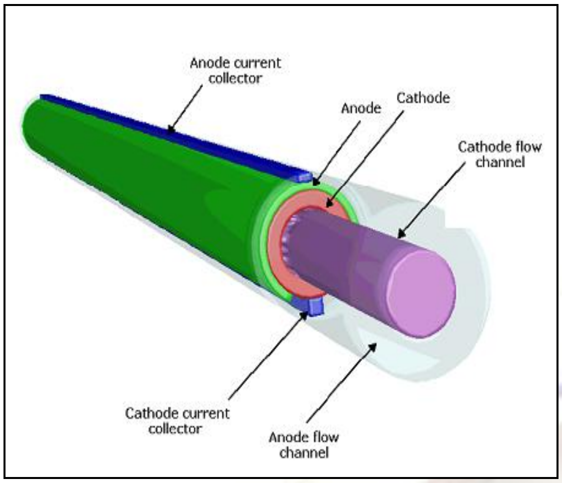

Fig. 4 Schematic of the Tubular SOFC problem

Hydrogen flows into the fuel cell on the anode side. It diffuses through the porous gas diffusion layers and comes in contact with the catalyst layer. Here it forms hydrogen ions and electrons. The hydrogen ions diffuse through the polymer electrolyte membrane at the center, the electrons flow through the gas diffusion layer to the current collectors and into the electric load attached. Electrons enter the cathode side through the current collectors and the gas diffusion layer. At the catalyst layer on the cathode side, the electrons, the hydrogen ions and the oxygen combine to form water.

In the fuel cell model in FLUENT, two electric potential fields are solved. One potential is solved in the membrane and catalyst layers. The other is solved in the catalyst layers, the diffusion layers, and the current collectors. Surface reactions on the porous catalyst region are solved and the reaction diffusion balance is applied to compute the rates. Based on the cell voltage that you prescribe, the current density value is computed. Alternatively, a cell voltage can be computed based on a prescribed average current density.

The Fuel Cell module is provided as an add-on module with the standard FLUENT licensed software. A special license is required to use the SOFC module. A fuel cell is an energy conversion device that converts the chemical energy of fuel into electrical energy. A schematic of a fuel cell is shown in Figure 3 & 4.

III. GOVERNING EQUATIONS

For conservation of mass,

$$\frac{\partial}{\partial x_j}(\rho u_i) = S_m \qquad \text{--- (1)}$$

On the cathode side, consumption of O_2 is assumed where source term, $S_m = -SO_2$ and

$$S_{O_2} = \frac{M_{O_2} i A_{cv}}{4F} \qquad \text{--- (2)}$$

On the anode side, the consumption of H_2 additional with the production of $H_2O(g)$ is occurred, giving $Sm = -S_{H2} + S_{H2O}$, where

$$S_{H_2} = \frac{M_{H_2} i A_{cv}}{2F} \qquad \text{--- (3)}$$

For conservation of momentum,

$$\frac{\partial}{\partial x_j}(\rho u_j u_i) = \frac{\partial p}{\partial x_i} + \frac{\partial \tau_{ij}}{\partial x_j} + S_{px_i} \qquad \text{--- (4)}$$

For conservation of energy

$$\frac{\partial}{\partial x_j}(\rho u_j C_p T) = \frac{\partial}{\partial x_i}\left(k \frac{\partial T}{\partial x_j}\right) + S_h \qquad \text{--- (5)}$$

In a fuel cell, chemical energy in the fuel is converted directly to electrical energy. However, part of the chemical energy is also converted to heat. It is considered that enthalpy of reaction is equivalent to heat released by electrical power plus the heat produced by irreversible processes such as heat generated from polarization effect. This irreversible heat production is regarded as a heat source term in the model and defined as,

$$S_h = \left(-\Delta H_{fH_2O}\right)\frac{iA_{cv}}{2F} - iA_{cv}V_{cell} \qquad \text{--- (6)}$$

There are additional equations used to solve for the mass flow rates of the species in the fluid flow whose local concentration is expressed as a mass fraction, m_m. The mass fraction is assumed to be governed by the mass transfer conservation equation for each species,

$$\frac{\partial}{\partial x_j}(\rho u_j m_A) = \frac{\partial}{\partial x_j}\left(\rho D_A \frac{\partial m_A}{\partial x_j}\right) + S_A \qquad \text{--- (7)}$$

The molecular diffusivity of component

$$J_{diff} = -D\left(\frac{dc}{dx}\right) \qquad \text{--- (8)}$$

Now, the gas diffusion of species I depends not only on the property of I but also the property of the species j through which I is diffusing. For this reason binary gas diffusion coefficients are typically written as D_{ij} where 'i' is diffusing species and 'j' is the species through which the diffusion is occurring. For binary system of two gases, D_{ij} is a strong function of temperature, pressure and molecular weights of species i and j. At low pressure, nominal diffusivity can be estimated from the following equation based on the kinetic theory of gases. [8]

$$pD_{ij} = a\left[\frac{T}{\left(T_{ci}T_{cj}\right)^{1/2}}\right]^{b}\left(p_{ci}p_{cj}\right)^{1/3}\left(T_{ci}T_{cj}\right)^{5/12}\left[1/M_i + 1/M_j\right]^{1/2} \quad \text{--- (9)}$$

In porous structure, the gas molecules tend to be impeded by the pore wall. The diffusion flux should be corrected to account for the effect of such blockage. Usually this is accomplished by employing a modified or effective diffusivity as per Burggemann correction, the effective diffusivity in porous structure can be expressed as. [9]

$$D_{ij}{}^{eff} = \varepsilon^{1.5} D_{ij} \quad \text{-- (10)}$$

Porosity represent ratio of pore volume to total volume which is normally 0.4 for fuel cell electrode.

If modified for include tortuosity 'τ'. [10]

$$D_{ij}{}^{eff} = \varepsilon^{\tau} D_{ij} \quad \text{--- (11)}$$

Potential Calculations

Cell voltage is calculated from the Nernst potential at equilibrium less losses from Ohmic, activation, and concentration polarizations. It is determined by

$$V_{cell} = E_N - iR - \eta_{act,a} - \eta_{act,c} - \eta_{conc,a} - \eta_{conc,c} \text{--- (12)}$$

Nernst potential and E^0 are defined by following equations

$$E_N = E^0 + \frac{RT}{2F} ln\left(\frac{P_{H_2a}P^{\frac{1}{2}}_{O_2a}}{P_{H_2Oa}}\right) \quad \text{--- (13)}$$

It is assumed that the stack operates at atmospheric pressure; therefore, the partial pressure terms are reduced to the gas species mole fraction terms in the calculations. Ohmic resistance is mainly due to the resistance to the flow of ions through the electrolyte, which is considered as a ratio of electrolyte thickness over the electrolyte conductivity, as shown in following equation. The Ohmic resistance in the electrode components is considered negligible in the light of their thin structure.

$$\eta_{ohmic} = j(ASR_{ohmic}) \quad \text{--- (14)}$$

Both activation and concentration polarizations are included in the model, and the activation polarization is found to be significant. These current density dependent terms are expressed in following equations.

$$\eta_{conc} = \frac{RT}{nF} ln\left(\frac{j_l}{j_l - 1}\right) \quad \text{--- (15)}$$

$$\eta_{act} = \frac{RT}{\alpha nF} lnj_0 + \frac{RT}{\alpha nF} lnj \quad \text{--- (16)}$$

IV. RESULT

Validation of present work is done by comparing its result of activation loss vs. current density with earlier study carry out by Chong Bo and Cai Bao [10]. Fig.5 shows that at low current density there is diversion between two results. At current density 1500 Amp / m2 the results closely appears to each other.

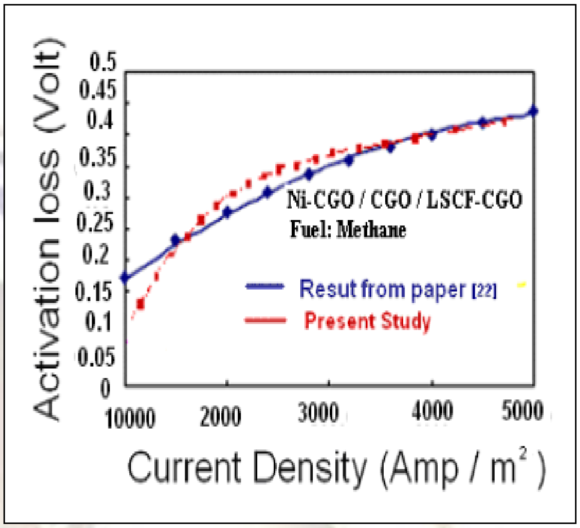

Fig.5 Current Density for Different Value of Activation Loss

Voltage Vs. current density for different material is given in Fig.6, which shows that voltage produce in Ni-CGO/ CGO / LSCF-CGO material composition is highest. Voltage produce in Ni / LMnO$_3$ / YSZ is more than Ni-YSZ / ZrO$_2$ / LaMnO$_3$ but it is decreases faster than Ni-YSZ / ZrO$_2$ / LaMnO$_3$ with increasing current density.

After current density equal to 1500 to 3500 Amp / m^2 the value of obtain from numerical are having lower value than experimental results. From current density 3500 amp / m^2 and higher the results are nearly same for both case.

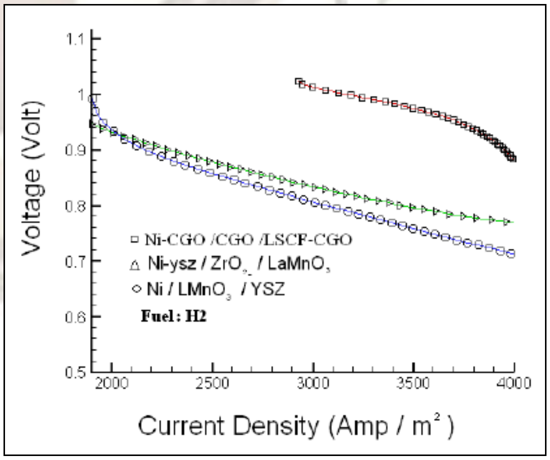

Fig.6 Effect of Current Density on Voltage

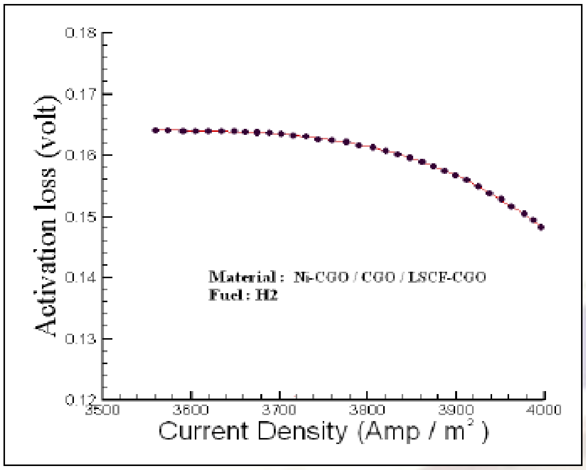

Fig.7 Variation of Activation Loss with Respect to Current Density

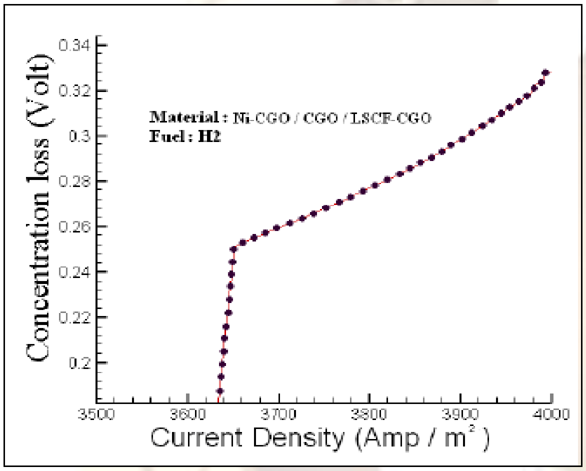

Fig.8 Variation of Concentration Loss With Respect to Current Density

Activation loss and concentration loss play major role in voltage production in TSOFC. Activation loss vs. Current density and Concentration loss vs. Current density are given In Fig.7 and Fig.8 respectively. Fig.7 shows that activation loss reduces with current density increases and Fig.8 shows that Concentration loss will increase with increasing current density. Activation loss will reduce on higher current density and concentration loss will become more significant on higher current density.

Temperature has significant effect on activation loss and concentration loss which are given in Fig.9 and Fig.10 respectively. This shows concentration loss is more significant then activation loss at high temperature. Activation loss will decrees at high temperature and high current density. When concentration loss is will incise at high temperature and high current density.

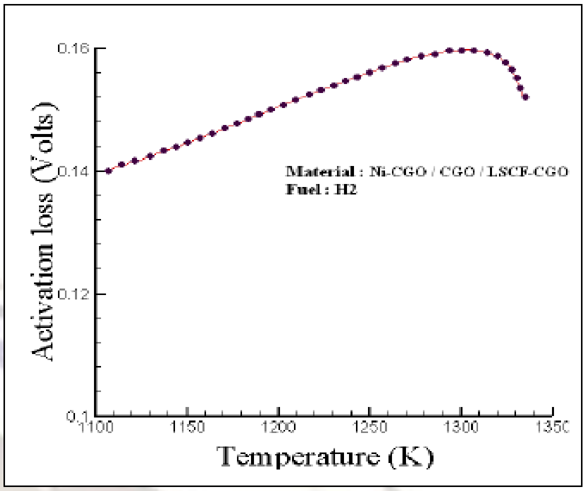

Fig.9 Variation of Activation Loss with Respect to Temperature

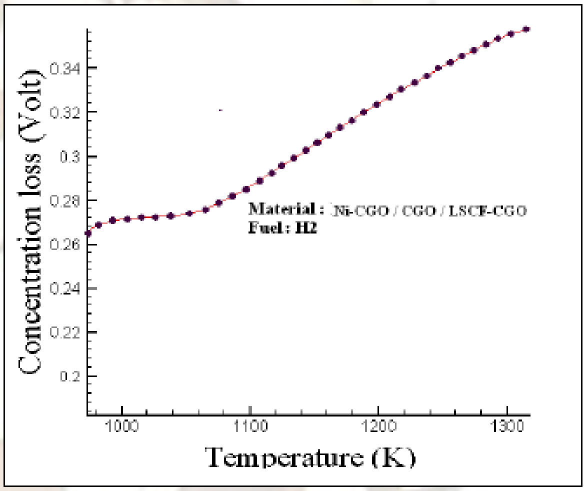

Fig.10 Variation of Concentration Loss with Respect to Temperature

Fig.12 shows that pure hydrogen can produce more voltage than methane or any other hydrocarbon use in SOFC as a fuel because above 979 K temperature gas shift reaction take place in hydrocarbon it will produce carbon monoxide as byproduct. Fig 11 represents performance of fuel cell; maximum power produce is 3575 W / m^2.

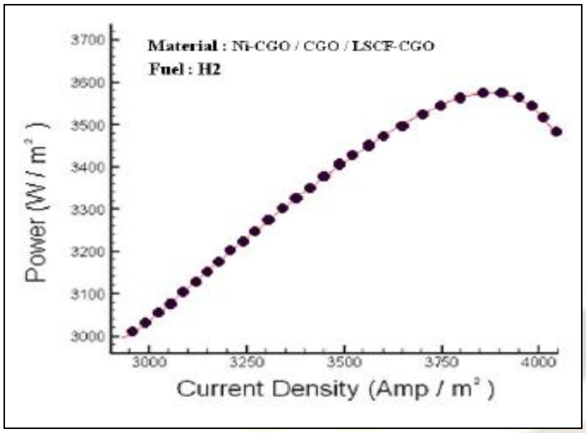

Fig.11 Performance of Fuel Cell

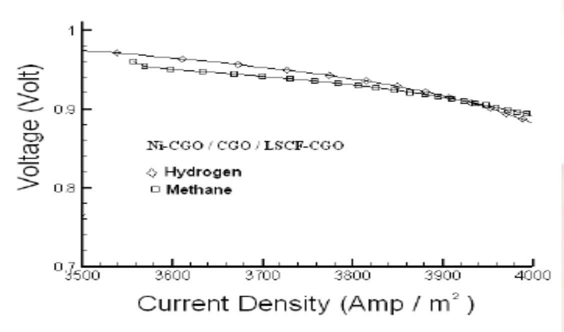

Fig.12 Variation of Voltage for Methane and Hydrogen as Fuel

V. CONCLUSION

The study leads following important conclusions.

1. By assign material composition Ni-CGO / CGO / LSCF-CGO. Performance gives better as compare to another two material composition Ni / LMnO3 / YSZ and Ni-YSZ / ZrO2 / LaMnO3 use for SOFC. Voltage produces by Ni-CGO / CGO / LSCF-CGO is 0.98 volt and maximum power produce 3575 W / m2.

2. Temperature is important parameter for performance of fuel cell.3. A concentration loss is more significant than activation loss.4. Methane show promising feature as a fuel for fuel cell.

REFERENCES

1. S. Ahmed, C. McPheeters, R. Kumar, "Thermal-hydraulic model of monolithic solid oxide fuel cell," J. Electrochem. Soc., 138, No. 9, September (1991).
2. J. Hartvigsen, S. Elangovan, A. Khandkar, "Modeling, design, and performance of solid oxide fuel cells," Proc. Of Zirconia V (1992).
3. H. Karoliussen, " Matematisk modellering av fastoxid braenslecelle," Ph.D. thesis, Department of Technical Electrochemistry, Norway Institute of Technology, Trondheim (1993).
4. P.G. Debendetti, C.G. Vayenas, "Steady-state analysis of high temperature fuel cells," Chemical Engineering Science, 38, No.11, (1983) pp.1817-1829.
5. M.D. Lukas, K.Y. Lee, H. Ghezel-Ayagh, IEEE Trans. on Energy Convers., 14, No.4 December (1999).
6. J. Domergue, A.Rufer, N.Buchheit, "Dynamic model of a solid oxide fuel cell stack and power converter," Proc. Of the 3rd European SOFC Forum, June 2-5, Nantes, France (1998).
7. A. Comte, Ph. Mathevon, Ph. Stevens, "Simulation of a solid oxide fuel cell using a dynamic system model," Proc. Of the 3rd European SOFC Forum, June 2-5, Nantes, France (1998).
8. Hirano, A., Suzuki, M., and Ippommatsu, M., 1992, "Evaluation of a New Solid Oxide Fuel Cell System by Non-isothermal Modeling," J. Electrochem. Soc., 139[10], pp. 2744–2751.
9. Achenbach, E., 1994, "Three-Dimensional and Time-Dependent Simulation of a Planar Solid Oxide Fuel Cell Stack," J. Power Sources, 49, pp. 333–348.
10. Chong Bo, Cai Bao, Chun Yuan, Xiang Zhao, "Parametric analysis of solid oxide fuel cell" Clean Tchnology And Enviromental Policy, Volume 11, Number 4, 391-399.